Journal of Non-Crystalline Solids 447 (2016) 167–170

Contents lists available at ScienceDirect

Journal of Non-Crystalline Solids

journal homepage: www.elsevier.com/locate/jnoncrysol

The effect of introduction of carbon on the glass forming ability and magnetic properties of melt-spun Fe-Si-B-Cu-C alloys

J. Xu, Y.Z. Yang *, W. Li, X.C. Chen

Faculty of Materials and Energy, Guangdong University of Technology, Guangzhou 510006, China

ARTICLE INFO

Article history:
Received 15 March 2016
Received in revised form 1 June 2016
Accepted 5 June 2016
Available online 10 June 2016

Keywords:
Amorphous-forming ability
Fe-based amorphous alloys
Soft magnetic materials
High saturation magnetic flux density

ABSTRACT

The effect of the minor addition of carbon on the amorphous forming ability and soft magnetic properties for the $Fe_{83.5-x}Si_2B_{14}Cu_{0.5}C_x$ (x = 0, 0.1, 0.2, 0.3, 0.4, 0.5) alloys were investigated. With the addition of minor C in $Fe_{83.5}Si_2B_{14}Cu_{0.5}$, the amorphous forming ability and the soft magnetic properties are improved clearly. The phase structure identified by XRD reveals that minor C addition inhibits the surface of crystallization and improve its amorphous-forming ability, when x = 0.2 and x = 0.3, a fully amorphous alloys were successfully obtained. All the as-quenched Fe-Si-B-Cu-C alloy ribbons show two separated distinct exothermic peaks from DSC curves. The addition of minor C element is contributed to increase the onset temperature of crystallization and a better thermal stability of the amorphous alloys. VSM and DC-BH loop tracer measurements show that the $Fe_{83.3}Si_2B_{14}Cu_{0.5}C_{0.2}$ amorphous alloys exhibit saturation magnetic flux density of 151.5 emu/g and low Hc of 4.0 A/m, respectively. By annealing, these amorphous alloys exhibit higher saturated magnetization. Low material cost and excellent soft magnetic properties make the FeSiBCuC alloys promise soft magnetic materials for industrial applications.

1. Introduction

The development of soft magnetic alloys has been noticed a variety of electromagnetic applications such as sensors, transformers, motors, actuators, and electronic and power devices, especially for energy saving [1–3]. These alloys have attracted great attention due to their excellent soft magnetic properties combining high saturation magnetization (B_s), high effective permeability (μ_e), low coercivity (H_c) and low core loss (W). Unfortunately, there are few amorphous/nanocrystalline alloys that at the same time satisfy a core loss (P) lower than that of grain oriented steel and B_s approaching that of the grain oriented steel. It is important to search for a new alloy with superior structural and functional properties, since this alloy can contribute to the sustainable development of human society and maintenance of the global environment [3–5]. The previously mentioned studies have found that a fine dense distribution of nanocrystals can be achieved in Finemet $Fe_{73.5}Si_{13.5}B_9Cu_1Nb_3$ [5]. As we all know that the small addition of Cu to the Fe-Si-B alloy results in clusters acting as potent nucleation sites for the α-Fe nanocrystals, while Nb element restricts coarsening of these nanocrystals [6]. Thus these alloying additions result in lower coercivity but have relatively low saturation magnetic flux density, B_s of 1.5–1.6 T. These can be attributed in part to the lower concentration of Fe in Finemet [6–11]. And with the addition of Cu element in FeSiB system, it is difficult to use in the current production machines due to their low amorphous forming ability [12–15]. Therefore, it poses a serious challenge to develop methods further increase the Fe content, improve amorphous forming ability and choose a new composition concurrently. Recently, low cost Fe-based nanocrystalline soft magnetic alloys with high saturation magnetic flux density Bs based on FeSiBCuP have been reported [16–20]. Although this alloy has shown many advantages, there are still some deficiencies that need to be solved. For example, the P element makes the alloy easy to be oxidized and difficult to control, which leads to high demand for vacuum. Thus, it limits their application [21,22].

So in this paper, with the aim at increasing glass forming ability and magnetic properties of $Fe_{83-83.5}Si_2B_{14}Cu_{0\cdot5}C_{0-0.5,}$ and melt-spun alloys were developed, which are free from expensive metal elements such as Nb, Zr, Mo, and are not contained volatile P element. The effect of minor C addition on amorphous forming ability, magnetic properties and the phase structure in FeSiBCuC alloy system are explored.

2. Materials and methods

Multicomponent alloy ingots with nominal compositions of $Fe_{83.5-x}Si_2B_{14}Cu_{0.5}C_x$ were prepared by high frequency induction, and melting the mixtures of low-cost raw materials Fe (99.9 mass%), Si (99.99 mass%) Fe-20 mass% B, Cu (99.9 mass%) and C (99.9%) under a high-purity argon atmosphere. The ingots were inverted and remelted four times to ensure homogeneity. Melt-spun ribbons were prepared by a

* Corresponding author.
E-mail address: yangyzgdut@163.com (Y.Z. Yang).

http://dx.doi.org/10.1016/j.jnoncrysol.2016.06.011
0022-3093/

single roller melt-spinning method with roller wheel speed of 50 m/s. Ribbons had a width of about 1 mm and a thickness of 25 μm. The as-quenched ribbons were annealed at various temperature for 600 s under nitrogen atmosphere. The structure of as-quenched ribbons were examined by X-ray diffractometer (XRD) with CuKα radiation. The thermal stability of the melt-spun ribbons were examined by differential scanning calorimeter (DSC) at a heating rate of 20 K/min, under nitrogen atmosphere. Crystallization onset temperature (T_x) and peak temperature (T_p) were determined from DSC curves. Saturation flux density (M_s) was measured with a vibrating sample magnetometer (VSM) under a maximum applied field of 15,000 Oe. A DC-BH loop tracer with the maximum applied field of 800 A/m was used to measure the coercivity Hc.

3. Result and discussion

3.1. Structural analysis

Fig. 1 shows the XRD patterns of all the as-quenched ribbons. The XRD measurements were performed on the roller wheel surface of ribbons. Only a broad peak at around $2\theta = 45°$ exhibiting an amorphous character was detected for the ribbons at Fig. 1(c) and (d), while a noticeable diffraction peak revealing a partial nanocrystallization appeared at around $2\theta = 65°$ corresponding to α-Fe for ribbons at Fig. 1(a), (b), (e), (f). It is not difficult to understand that the cooling rate of free surface is lower than the wheel surface, resulting in a surface crystallization behavior.

But with the addition of minor C element, the crystallization peak gradually weakens until disappears and the sample exhibits a typical halo diffraction peak, indicating the amorphous structure. As can be seen from the picture that the amorphous forming ability of Fe-Si-B-Cu-C alloy depends on the carbon content. Meanwhile, with further addition of C element, the crystallization peak reappears and is getting stronger. On the one hand, large negative mixing enthalpies among the constituent elements are benefit for a highly amorphous forming ability. The addition of C increases the alloys negative mixing enthalpy, which improves the alloys amorphous forming ability. On the other hand, the size of the difference between atoms may form highly packed atomic configuration and reinforced its original structure in the amorphous structure, resulting in suppressing grain growth. When $x = 0.2$ and 0.3, the addition of minor C make the alloys have a strong amorphous forming ability. Although the addition of C increases the atom size differences in the alloy and enhances the negative mixing enthalpy, AFA has not been improved. The reason may be that with the increase of C content makes the alloy composition deviate from the eutectic point of the alloy, which reduces the AFA [10–12].

Hence, the phase structure analysis indicated that addition of minor C inhibits the surface crystallization of $Fe_{83.5}Si_2B_{14}Cu_{0.5}$ and contributes to the improvement of its amorphous forming ability.

3.2. Thermal analysis

The presence of the amorphous phase was confirmed by DSC studies. As shown in Fig. 2, the DSC curves for the as-quenched $Fe_{83.5-x}Si_2B_{14}Cu_{0.5}C_x$ ($x = 0, 0.1, 0.2, 0.3, 0.4, 0.5$) alloy ribbons exhibit two exothermic peaks which means that there exists a two-step crystallization processes before the final stable phases are obtained. Obviously the crystallization occurs in two distinct stages corresponding to the nanocrystallization process of α-Fe. The characteristic temperatures of T_{x1} and T_{x2} in all DSC curves were noticed. The first broad peak (T_{x1}) corresponds to the precipitation of the α-Fe solid solution from the amorphous phase and the second sharp peak (T_{x2}) corresponds to the formation of Fe-B compounds [16–19].

It was also observed in the DSC data that the first crystallization reached the maximum about at 452.2 °C when 0.3 at.% carbon was added to Fe-Si-B-Cu alloys. All the as-quenched ribbons indicate that the T_{x1} gradually decreased and $\Delta T_x = T_{x2} - T_{x1}$ gradually widened with the increase of C, but for $Fe_{83.3}Si_2B_{14}Cu_{0.5}C_{0.2}$ and $Fe_{83.2}Si_2B_{14}Cu_{0.5}C_{0.3}$. With the changing of x, there is no effect on T_{x2} and T_{p2}. As it is well known, the crystallization onset temperature is related with the nucleation process, and the peak temperature is associated with the growth process. Therefore, the results imply that C content up to 0.2–0.3 at.%, makes nucleation and growth more difficult, thus improving its thermal stability [20–23]. For the Fe-Si-B-Cu-C alloy system, the T_{x1} gradually decreased and the temperature difference (ΔT_x) between T_{x1} and T_{x2} expands, to some extent, reflecting that the $Fe_{83}Si_2B_{14}Cu_{0.5}C_{0.5}$ alloy exhibits a large annealing temperature range, which is advantageous for synthesizing nanocrystalline alloy with good soft magnetic properties. Detailed results of the DSC curves are summarized in Table 1.

3.3. Magnetic properties

Fig. 3 illustrates the magnetic hysteresis loops for the Fe-Si-B-Cu-C alloys. Fig. 4 shows the dependence of saturated magnetization (Ms) on carbon content.

It can be seen that Ms increases from 150.5 emu/g to 187.5 emu/g as Fe content increases from 83 at.% to 83.5 at.%, proving that high Fe

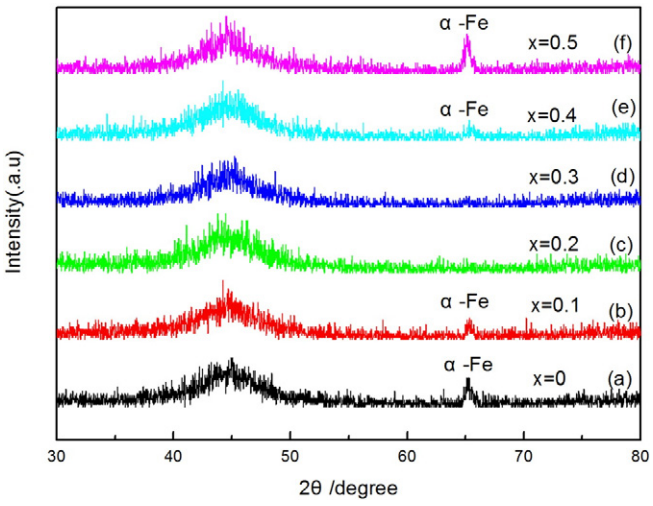

Fig. 1. XRD patterns of various $Fe_{83.5-x}Si_2B_{14}Cu_{0.5}C_x$ ($x = 0, 0.1, 0.2, 0.3, 0.4, 0.5$) melt-spun ribbons.

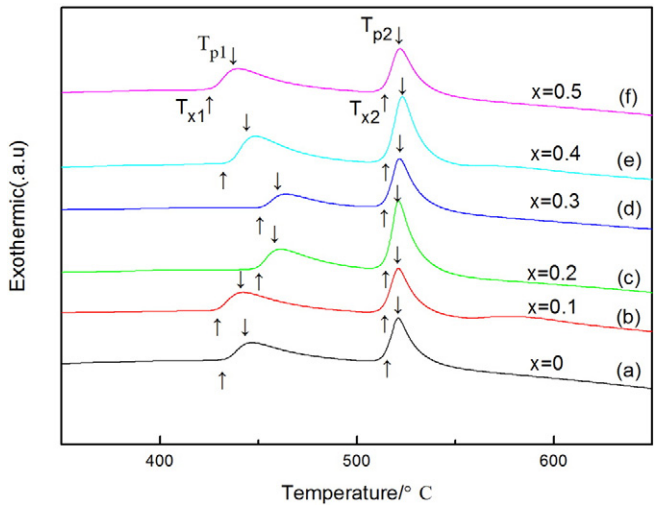

Fig. 2. DSC curves at a heating rate of 20 K/min for $Fe_{83.5-x}Si_2B_{14}Cu_{0.5}C_x$ ($x = 0, 0.1, 0.2, 0.3, 0.4, 0.5$) melt-spun ribbons.